5-2011

The Applications of Graphene and Its Derivatives for Heavy Metal Removal

Clemonne John Madarang

MONTCLAIR STATE UNIVERSITY

The Applications of Graphene and Its Derivatives for Heavy Metal Removal

by

Clemonne John Madarang

A Master's Thesis Submitted to the Faculty of

Montclair State University

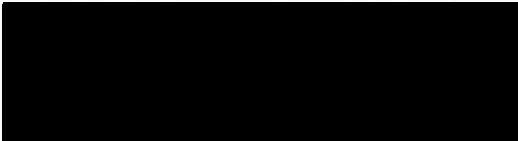In Partial Fulfillment of the Requirements

For the Degree of

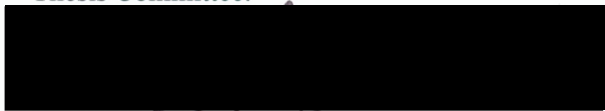Master of Science in Chemistry, Concentration in Biochemistry

May 2011

College of Science and Mathematics

Department of Chemistry and Biochemistry

Robert Prezant, PhD.
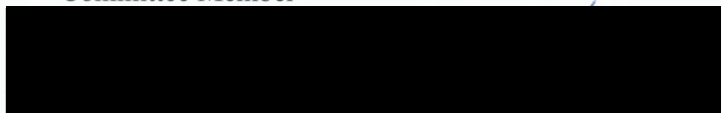Dean of College of Science and Mathematics

5/12/11
Date

Thesis Committee:

Shifeng Hou, PhD.
Thesis Sponsor

John J. Siekierka, PhD.
Committee Member

Huan Feng, PhD.
Committee Member

Marc L. Kasner, PhD.
Department Chair

Abstract

Heavy metal pollution is very prevalent in our environment. The entire removal of heavy metal and organic contaminants in natural water resources will not only affect the environment itself, but also can block the toxic contaminant transfers in food chains. Currently, there are many studies being done to remove these heavy metal ions from our water, such as reduction reactions, chemical precipitation, reverse osmosis and electrolytic recovery. One of the promising techniques is adsorption. The focus of this research is using graphene and its derivatives, such as silylated graphene oxide (GO), to adsorb heavy metals, specifically, lead. This research describes chemical modification techniques to modify the GO surface with functional groups, and the modified graphene will be used as a functional sorbent for waste water treatment and natural water resource protection, especially for heavy metal removal. In this study, N-(trimethoxysilylpropyl) ethylenediaminetriacetic acid (EDTA-silane) was linked to the graphene oxide (GO) surface through a silanization reaction. EDTA is a widely used chelating agent, and modifying the surface of GO with EDTA will add a chelating ability to GO. The results demonstrate that the EDTA-GO compound is an ideal adsorbent for heavy metal removal with a higher adsorption capacity than the carbon-based adsorbents currently in use. EDTA modification enhanced the adsorption capacity of GO due its chelating ability. At pH 6.0 ~7.2, the adsorption capacity for Pb(II) removal was found to be 486 mg/g, with adsorption completed within 20 minutes. A Langmuir adsorption model agrees well with experimental data. The effects of solution conditions such as pH and metal ion concentrations were investigated, along with adsorption and desorption behaviors of heavy metal cations. The desorption behavior predicts that GO can be reused after washing with 0.10 M HCl. My results have demonstrated potential applications for uses in the environmental restoration.

Keywords: *Graphene Oxide, EDTA, heavy metal adsorption*

The Applications of Graphene and Its Derivatives for Heavy Metal Removal

A Thesis of Master Degree

Submitted in partial fulfillment of the requirements

For the degree of Master of Science in Chemistry

By

CLEMONNE JOHN MADARANG

Montclair State University

2011

Table of Contents

1. Introduction

1.1 Heavy Metal Problem

There is a worldwide concern for the pollution of water. The world's water resources are being polluted due to the improper disposal of toxic metals and organic pollutants. Excess metals such as cadmium, chromium, copper, lead, mercury and zinc are an environmental concern, and need to be removed from the water, mainly because of their toxicity. The metal ions come from wastewater discharged by many industries such as metallurgy, tannery, chemical manufacturing, mining, battery industries. If the wastewater from these industries is left untreated, these metal ions find their way into our food chain through the waste that discharges into the bodies of water [1]. Consumption of these metals result in nausea, convulsions, coma, renal failure, cancer and even subtle effects on metabolism and intelligence [1]. Heavy metals are non-biodegradable and can accumulate in living tissues, posing a threat to living species [2]. There is a worldwide concern to minimize, if not remove, heavy metals contaminating our water systems.

The continuous increase of the world's population has raised the demand for clean water. In addition to the health of the world's population, clean water is a critical resource for a variety of key industries, including electronics, pharmaceuticals and of course, food [3]. The world is facing incredible obstacles in meeting growing demands of clean water, as the available supplies of freshwater are decreasing due to extended droughts, population growth, more stringent health based regulations.

1.2 Existing Techniques

Techniques are being applied to remove these metal ions from the water, such as reduction reactions [1], chemical precipitation, and electrolytic recovery [4]. Chemical precipitation involves the addition of a base, such as NaOH or $CaCO_3$ to a solution of heavy metal contaminated water. The addition of this base reacts with the metal ions in the solution and precipitates a metal salt. This is very useful for high concentrations of heavy metal contamination. Reduction reactions and electrolytic recovery are similar to each other in that both methods make use of an electric current to remove the heavy metal contamination in the solution. Among the above methods, the promising process for the removal of metal ions from water and wastewater is in adsorption [2].

1.3 Adsorption Mechanism and Sorption Models

Adsorption is a reaction process that occurs on the solid surface of the adsorbent that interacts with heavy metal ions and pollutant molecules. The efficiency of the adsorbent to be able to adsorb the pollutants depends strongly on adsorbent's surface properties, chemical composition, surface charges and surface area. It is a surface phenomenon that involves the adhesion of atoms, ions or molecules in solid, liquid or gaseous phase to a surface. The phenomenon occurs due to a consequence of weak interactions between the adsorbate and the adsorbent. If the attractive forces of the adsorbent and the adsorbate are greater than the cohesive energy keeping the adsorbate together, the adsorbate will drive towards a state of lower free energy. The bonding that occurs between the adsorbent and the adsorbate can be due to Van der Waals forces (physisorption), covalent bonding (chemisorption) or electrostatic forces. The adsorption

process is reversible, and the employed adsorbent can be regenerated by suitable desorption process.

The mechanism of interactions of adsorbent and adsorbate are not homogenous all across the solid surface, requiring the use of sorption isotherm models to help explain and describe the adsorption process. There are two adsorption isotherms used in this study, the Languir adsorption isotherm and the Freundlich adsorption isotherm. Both equations and theorems will be discussed further, in the results section.

With these models, the data acquired by doing adsorption experiments can be explained and reasonably compared among various sorbents, to help researchers have informed decisions on the next novel technology for adsorption processes.

1.4 Examples of Adsorbent Material

With increasing demands for treating heavy metal environmental problems, the development of high performance sorbents is an important research area [4]. The composition, quality, physical and chemical properties and even the rarity of the raw material are all factors that are taken into account when studying a novel adsorbent. There are a variety of resources used for adsorbents, such as coconut husks [6,7], charcoal [8], and even lichens and bacteria [10,11,12,13]. Each resource has its own unique characteristics that give it both advantages and disadvantages over the other possible adsorbents.

Peanut hull husks are a possible option as a sorbent [9]. Brown, et. al. (2000) investigated the use of peanut hull husks as an adsorbent for Cu^{2+}, Cd^{2+}, Zn^{2+} and Pb^{2+} compared to raw peanut hulls to find a low-cost alternative for using commercial grade ion-exchange resin. Although the investigation proved that peanut hull husks are

effective adsorbents, the husks have a much lower capacity than the commercial grade resin.

Biosorption is another method where researchers have been discovering new adsorbents. This technique involves the use of biomass or biofilm to adsorb heavy metal ions and other contaminants in aqueous solutions [10,11]. Most of the biomasses used are different species of fungi and algae, which can then adsorb heavy metals through a very complex mechanism. One advantage to having these biosorbents is that they are quite effective in removing heavy metals from a wastewater streams that have a low concentration of heavy metal ions. The idea of biosorption is still quite novel, and additional research is being done to understand the mechanism and process through which these biosorbents work.

Other adsorbents that have been used for adsorption of metal ions such as activated carbon [14, 15, 16], and PVA beads [17] are not very effective. Some of these adsorbents suffer from low adsorption capacities or low removal efficiencies of metal ions. Therefore, scientists are still being driven to discover promising new adsorbents. An ideal sorbent should have the ability to remove toxic contaminants from environments to a safe level while doing so rapidly and efficiently. Tremendous effort has been made in recent years to seek new sorbents. Discovering new and effective adsorbents using carbon based nanomaterials are becoming more popular because they prove to be very versatile for use in dealing with mineral and organic pollutants.

1.5 Carbon Nanomaterials and Carbon Nanotubes

The development of novel nanomaterials with increased affinity, capacity, and selectivity for heavy metals and other contaminants as an adsorbent is an emerging

research area. The benefits from the use of nanomaterials may derive from their enhanced reactivity, increased surface area and removal characteristics. The advantages of nanoparticles as attractive sorbents are that they have much larger surface areas than bulk particles, can be functionalized with various chemical groups to increase their affinity towards target compounds [18]. These functionalization techniques can be performed directly on the nanoparticle surface. The smaller the particle size, the higher the specific area of the particle is for interacting with chemical adsorbates. Besides the size of the sorbents, the adsorption properties are highly dependent on surface groups and surface charges. A variety of nanomaterials are in various stages of research and development, each possessing unique functionalities that are potentially applicable to the remediation of industrial effluents, groundwater, surface water and drinking water [19].

Carbon nanotubules are tubes made up of rolled up graphene sheets [20]. Since their discovery in 1991, carbon nanotubules (CNTs) have attracted great attention because of their unique properties [21]. CNTs have become a foundation for future applications to nanodevices, field emission, gas adsorption [22], composite reinforcement, metal nanocomposites and catalyst supports [23], as they possess exceptional mechanical properties, unique electrical properties, high chemical and thermal stability and a large specific surface area. CNTs have been used for the determination of heavy metal ions in aqueous environments because CNTs are an effective adsorbent due to their porous and graphitic structure.

It has been shown that surface–attached functional groups such -COOH and-OH have stronger attractive forces toward metal ions than bare CNTs, and other carbon material surfaces [23]. These functional groups generate a rise in negative charge on the

carbon surface with oxygen atoms in functional groups donating a single pair of electrons to metal ions, consequently increasing their cation exchange capacity. The sorption capacities of metal ions by raw CNTs are very low, but are significantly increased after being oxidized by HNO_3, $NaOCl$, and $KMnO_4$ solutions.

1.6 Graphene and Its Derivatives (GO)

One interesting adsorbent that has a low cost with high efficiency is graphene. Graphene is a single layer of carbon atoms packed into a honeycomb-shaped lattice. It is derived from graphite, which is composed of multiple layers of these honeycomb-shaped lattices, as shown in Figure 1.
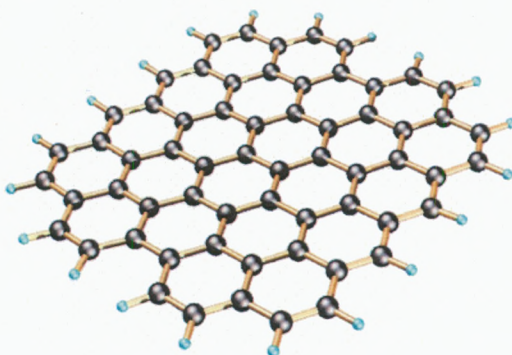
Figure 1. Idealized structure of a single layer of graphene

Graphene is the first free-standing two-dimensional atomic crystal that has been found so far. It exhibits many remarkable electronic and mechanical properties. Since its discovery in 2004 [26], graphene has become one of the most interesting topics in the area of materials science and has attracted significant attention from scientists in diverse fields such as chemistry and physics. Graphene has taken the center stage of research in many critical areas due to its unique properties which include superior mechanical strength, low density and high heat conductance. These unique physical and chemical properties make it promising for potential applications in many fields including

nanoelectronics [27], sensors, nanocomposites, batteries and fuel cells, super-capacitors and hydrogen storage [28].

When graphene is chemically oxidized, it exists in two oxidation states: graphene oxide (GO) and reduced graphene oxide (RG). The oxidation of graphene creates numerous oxygen-containing functional groups at the surface of graphene, such as hydroxyl, epoxy, carbonyl and carboxyl groups, which together make the graphene surface polar [27]. GO (Figure 2) is water soluble with low conductivity while RG has good conductivity with poor solubility in water. The solubility of GO in water and other solvents allows it to be uniformly deposited onto wide ranging substrates, such as thin films [29]. The abundant functional groups on the surfaces of GO can be used as anchoring sites for metal nanoparticles, making it possible to use them as a support for producing graphene nanoparticle hybrids. Combinations of graphene and functional nanoparticles may lead to materials with interesting properties for a variety of applications.

Figure 2. Idealized structure proposed for graphene oxide (GO). Adapted from C. E. Hamilton, PhD Thesis, Rice University (2009).

GO has been tested as a potential adsorbent for various organic materials such as humic acid [31], ammonia [32], alcohols, aromatics and chloride compounds [33]. In each of these cases, GO has been proven to be a better adsorbent than the previous standard being used. These results further encourages our investigations to focus on developing GO as a good lead for developing a novel adsorbent for heavy metals.

1.7 Idea of EDTA-GO

This thesis describes methods to introduce modify the GO surface to make the adsorbent that much more efficient. If the objective of the adsorbents is to bind heavy metals, then a chelating agent should greatly increase the functionality of GO. This thesis will discuss the effects of modifying the GO surface with Ethylenediaminetetraacetic acid (EDTA) how this novel nanomaterial, EDTA-GO, can used to develop better adsorbents in the future.

2. Materials and Methods

2.1 Synthesis of graphene oxide

Graphite purchased from Sigma-Aldrich was used for the preparation of graphene oxide by a modified Hummers' method. Graphite powders were first oxidized by sulfuric acid. Then 5 g of the graphite powder was first treated with a solution by mixing 25 ml of concentrated H_2SO_4 with 5 g $K_2S_2O_8$ and 5 g P_2O_5. The mixture was kept at 80 °C for 6 hours using a hotplate. Subsequently, the mixture was cooled to room temperature and diluted with 1.0 L of de-ionized (DI) water and left overnight. The mixture was then

filtered and washed with de-ionized (DI) water to remove the residual acid. The product was dried under ambient conditions overnight. The pre-oxidized graphite was then subjected to oxidation by Hummers' method. The pretreated graphite powder was put into 250 mL of concentrated H_2SO_4 at 0 °C. Then 30 g of $KMnO_4$ was added gradually to the acid solution with stirring, while the temperature of the mixture was kept below 20 °C by cooling. The mixture was then stirred at 35 °C for 4 hours and then diluted with 500 mL of DI water. Because adding water to concentrated sulfuric acid medium releases a large amount of heat, the dilution was carried out in an ice bath to keep the temperature below 50 °C.

After adding all of the 500 mL of DI water, the mixture was stirred for 2 hours, and then an additional 1.5 L of DI water was added. Shortly thereafter, 40 ml of 30% H_2O_2 was added to the mixture, and the color of the mixture changed into brilliant yellow and began bubbling. The mixture was filtered and washed with 0.1 M HCl to remove metal ions, followed by 1.0 L of DI water to remove the acid. The produced GO solid was dried in air at room temperature.

2.2 Silylation of graphene oxide

To silanize GO, 10 mg of GO was added to a three-neck flask with 50.0 mL of ethanol and dispersed through ultrasonication for 60 min. Then 5 mL of a 1.0 wt% ethanol solution of N-(trimethoxysilylpropyl) ethylenediamine triacetic acid (EDTA-silane) was added and stirred for 12 hours at 60–65 °C for silylation. After the reaction finished, 100 mL of methanol was added to dilute the unreacted silane molecules. The product (EDTA-GO) was obtained by filtration and washed with methanol and water sequentially.

To reduce EDTA-GO to EDTA-RGO, 100 mg of EDTA-GO was dried in a vacuum oven at 80 °C for 12 hours and then dispersed into 50 mL of DI water and reduced with hydrazine by a previously published method [37]. Upon reduction, the solution changed from brown to black in color. The product EDTA-RGO was obtained by filtration, then washed with methanol, water and HCl sequentially and oven-dried for further use.

2.3 Heavy Metal Solutions

The Pb^{2+} solution used in these experiments has a concentration of 1 mg/mL. To make this solution, 0.673 g of $PbCl_2$ was added to 500 mL of Di H_2O in a plastic bottle. Aside from these, 1 mg/mL solutions of Ca^{2+}, $Cd^{2+,}$ Co^{2+}, Cu^{2+}, Mg^{2+} and Ni^{2+} were made using the same method. Solutions were prepared at All of the metal salts were obtained through Sigma-Aldrich.

2.4 Characterization of EDTA-GO and EDTA-RGO

Fourier transform infrared (FTIR) spectrometry, X-ray photoelectron spectroscopy (XPS) and field emission analytical transmission electron microscopy (TEM) were used to characterize the changes in structure and surface morphology of the graphene after each treatment step. For FTIR (Perkin Elmer Spectrum One, USA), EDTA-RGO, EDTA-GO, GO and RGO were separately pressed into pellets with potassium bromide and then scanned from 500 cm^{-1} to 4000 cm^{-1} at a resolution of 4 cm^{-1}. The SEM images were taken on a Hitachi S-3400N scanning electron microscope with a Bruker X-flash X-ray microanalysis system. In the XPS analysis (surface analysis PHI5600, Physical Electronics Inc.), a monochromatic Al–Ka X-ray was used at 14 kV. The UV–Vis spectra were acquired with a Thermal Fisher Evolution 300 instrument.

2.5 The Adsorption Experiments

A typical adsorption experiment was performed by mixing 20 mg of EDTA-GO with a 100 mL Pb(II) ion solution. The initial metal ion concentrations vary from 5 ppm to 100 ppm, while the pH value of all Pb(II) ion solutions was maintained at 7.2 with NH_4Cl-NH_3 buffer solution. The solution was left with a given time. At the end of the given contact time, the mixture was filtered rapidly with 0.2μm membrane. The metal ion concentration in the filtrate was determined by AA spectroscopy, UV-Vis spectroscopy and ICP-MS. The amount of metal ions adsorbed by the adsorbents was taken as the difference between the initial and final ion concentration of the solutions and the adsorption capacity (q_e, mg/g) of the Pb(II) adsorbed onto EDTA-GO sorbent was obtained on the basis of the following equation:

$$q_e = \frac{(c_i - c_f) \times V}{w} \qquad (1)$$

where C_i and C_f are the initial and final (equilibrium) concentrations (mg/ml) of the Pb(II) in the solution, respectively, V (ml) is the volume of Pb(II) solution and w (g) is the weight of EDTA-GO sorbent.

The filtered EDTA-GO solid was investigated with SEM EDAX to identify the surface element components. The effects of pH on metal ions adsorption were measured with the same procedure mentioned above but the pH values of the solution were adjusted to 3.0, 4.5, 5.5, 7.2 and 8.2 with an HCl buffer solution.

2.6 The Desorption Experiments

To perform desorption process, the preloaded-Pb EDTA-GO samples were prepared through the same procedure mentioned above. The amounts of the loaded Pb(II) on EDTA-Go sorbent were calculated by the equation (2).

$$w_{ad} = \left(c_i - c_f \right) \times V \quad (2)$$

where C_i and C_f are the initial and final (equilibrium) concentrations (mg/ml) of the Pb(II) in the solution. After filtered and quickly washed with pH=7.2 buffer solution, dried in an oven, the Pb-pretreated EDTA-GO was mixed with 100ml pH=2.0, 30, 4.0, 5.0, 6.0 HCl solution and pH=7.0 DI water, respectively. After four hours treatment, Pb(II) adsorbed onto EDTA-GO surface was desorbed and dissolved into HCl solution. Then the solution was filtered through a membrane and washed with pH=7.2 buffer solution quickly. The filtered solution was carefully collected, diluted to 250.0 ml, and used to test the desorption amount of Pb(II) from EDTA-GO adsorbent. After dried in an oven, the filtered HCl-washed EDTA-GO solid was studied with SEM EDXs. The surface element ratio was calculated from the strength and the data reflect the surface element enrichment.

As a control experiment, other related carbon materials, graphite, activated carbon, GO, RGO, etc. were used to detect the adsorption and the desorption behavior in the same procedure mentioned above.

2.7 SEM and EDX Experiments

About 0.2 mg of graphene, GO and EDTA-GO were added to a small scintillation vial. X amount of 1 mg/mL $PbCl_2$ solution was added to the vials and the mixture was left on the bench top overnight. The mixture was then vacuum filtered through a 0.2 μm membrane, and the solid sample was collected and dried in a vacuum oven overnight. After the sample was dried, a small amount of the solid was placed onto a piece of copper tape that was then arranged on a disc for SEM analysis. Each sample was scanned at least three times at different cross sections of the sample under the SEM. The Bruker EDX program was used to take a snapshot of the scans done by the SEM instrument and also for the calculation of percent composition of the solid sample.

3. Results and Discussion

3.1 Characterization of GO, EDTA-GO and EDTA-RGO

3.1.1. FTIR Spectra

The FTIR spectra of the EDTA-RGO, EDTA-GO, GO and RGO are shown in Figure 3. The presence of carboxyl groups was identified with the appearance of a peak at 3421 cm^{-1}, which was observed for all four graphene samples, and with the presence of a peak at 1732 cm^{-1}, which is characteristic of the C=O stretching of both the carboxylic and carbonyl groups of graphene. The 1732 cm^{-1} peak was observed for all of the four graphene samples with almost the same strength and small shifts. This stable band suggests that the carboxylic or carbonyl groups of graphene were not reduced to C-OH. A weak signal at 1120 cm^{-1} for EDTA-GO and GO suggests the presence of an epoxy group on the graphene surface. Upon reduction with hydrazine, this peak disappeared for the EDTA-RGO and RGO samples, indicative that the reduction process converts C-O-C on

the graphene oxide surface to π-conjugation. This conclusion was also verified by energy dispersive X-ray data, which will be discussed later.

Upon modification with EDTA-silane, the presence of ionized carboxyl groups from EDTA chain was observed by the appearance of a new band at 1628 cm^{-1}. This band was observed for the EDTA-GO and EDTA-RGO samples only and with the same strength. The peak at 1732 cm^{-1}, which was assigned to the carboxylic groups of graphene, was observed for the EDTA-GO and EDTA-RGO surfaces without shift.

In addition to the bands of the carboxylic groups, additional new bands were observed on the EDTA-GO and EDTA-RGO samples. The band at 1162 cm^{-1} corresponds to the stretching vibration of Si-O-C and appeared in EDTA-GO. After reduction with hydrazine, this band shifted to 1096 cm^{-1}. The presence of two new bands at 2917-2800 cm^{-1} is associated with the stretching of the methylene groups from the EDTA-silane molecules. These two bands, combined with another new band at 1401 cm^{-1}, were contributed from the γ_{CH2} group of EDTA. The peak of EDTA-GO and EDTA-RGO at 1066 cm^{-1} was assigned to the formation of Si-O-C. The new peak at 2367 cm^{-1} was observed for EDTA-GO, but not for EDTA-RGO.
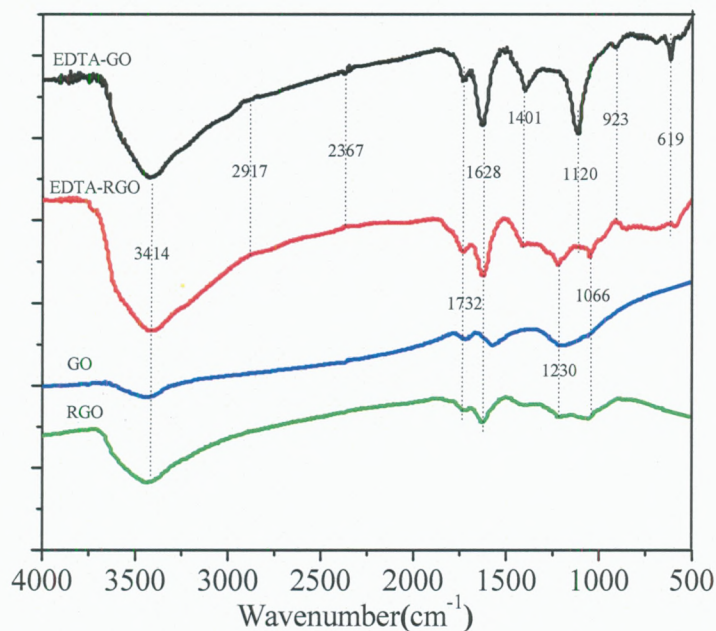
Figure 3. FT-IR spectra of GO, EDTA-GO and EDTA-RGO

3.1.2 XPS Spectra

Additional evidence for the existence of silane groups on graphene surface was seen in the XPS spectra (Figure 4). The silylation process was monitored by XPS of powders of GO, RGO, EDTA-GO and EDTA-RGO, separately. Comparison of the XPS spectra of EDTA-RGO and RGO (Fig. 4a) revealed the lack of a silicon signal in the RGO sample and the presence of a silicon signal (Si_{2p} 104.4 eV) in the EDTA-RGO sample. This proves the existence of silicon on the graphene surface.

The N_{1s} XPS data of EDTA-RGO were in accordance with the conclusions from the Si_{2p} XPS data. The N_{1s} XPS spectrum of RGO contained one peak at 401.2 eV, which was assigned to $N-C_{sp3}$ or $N-C_{sp2}$. Nitrogen was introduced to the graphene surface during the synthesis and reduction process. However, two peaks of N_{1s} were observed in

the EDTA-RGO sample: one is the same as that for RGO, and the other at 400.7 eV was presumably due to the tertiary amines of the EDTA.
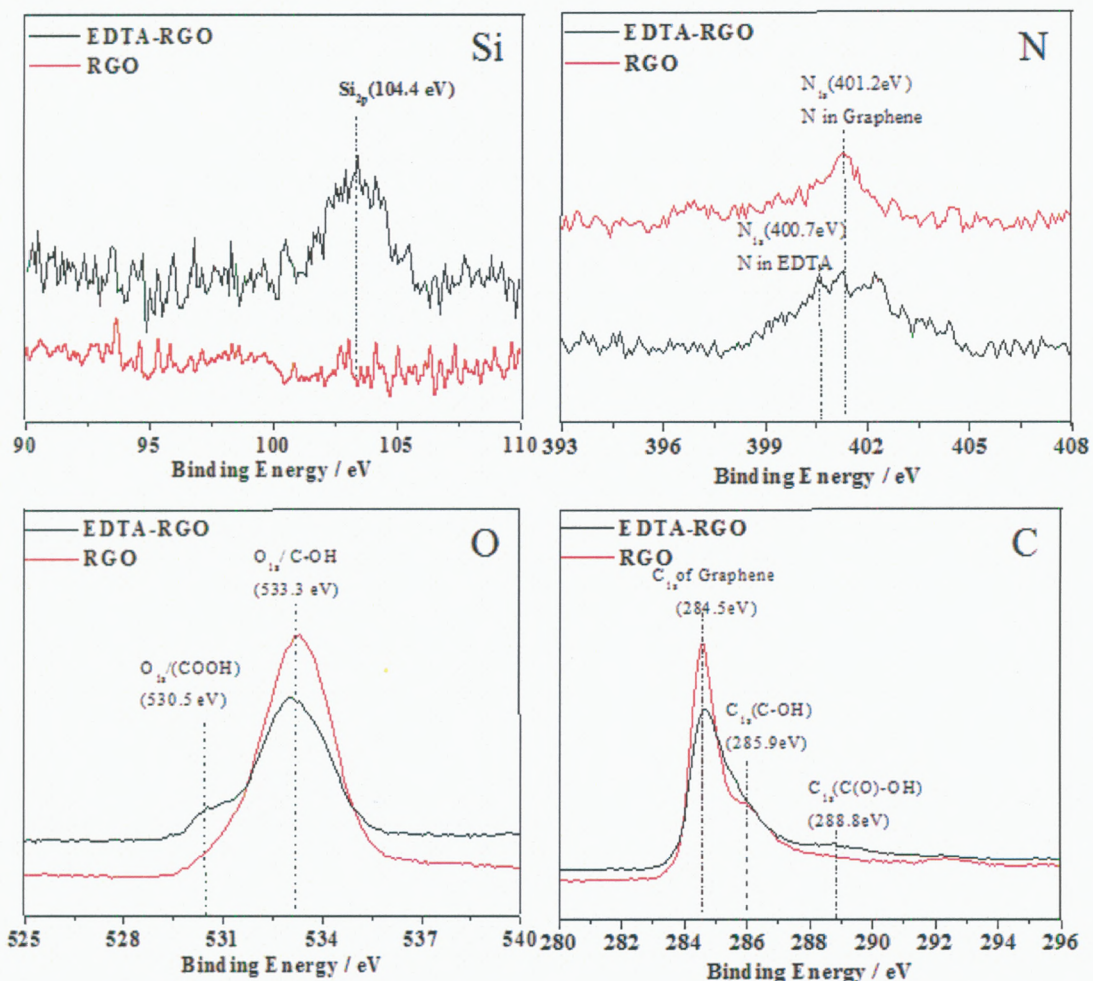

Figure 4. The XPS spectra of Si, N, O and C at RGO, EDTA-RGO

Two peaks in the O_{1s} spectra were observed for both RGO and EDTA-RGO. The O_{1s} peak at 530.5 eV was likely contributed from the carboxyl or carboxylic acid groups, and that at 533.3 eV was due to alcohol groups. In comparison to the O_{1s} spectrum of RGO, the EDTA-RGO sample clearly exhibited a peak with increased intensity corresponding to the carboxyl groups (530.5 eV). In addition, the stronger intensity of the carboxyl O_{1s} signal at 530.5 eV, along with a weaker peak of O_{1s} (C-OH) at 533.3 eV

from EDTA-RGO, demonstrated the presence of the –COOH groups of EDTA on the EDTA-RGO surface, and it also confirmed that part of the alcohol groups on the RGO surface were converted to C-O-Si groups through the silylation process.

The C_{1s} spectra of RGO and EDTA-RGO both contained main peaks at 284.5 eV, which were assigned to the binding energy of C-C and C-H of graphene. In addition, both RGO and EDTA-RGO have two other peaks. The peak at 285.9 eV was assigned to contributions from the C-OH groups, and the peak at 288.8 eV was due to the COOH groups. The peak intensity at 285.9 eV of EDTA-RGO was less than that of RGO, indicating that a considerable amount of C-OH had been converted to Si-O-C by the silylation process. In addition, the peak intensity at 288.8 eV of EDTA-RGO was much stronger than that of RGO, suggesting a considerable proportion of the carboxylic acid groups from EDTA bound to the graphene surface through the silylation process.

3.1.3 SEM Analysis of EDTA-GO and EDTA-RGO

Figures 5a and 5b show SEM images of the EDTA-GO and EDTA-RGO sheets on a gold surface. After the last reduction step, the lateral dimensions of EDTA-RGO ranged from several hundred nanometers to several micrometers. It appeared transparent and was folded over on one edge with isolated small fragments of graphene on its surface. These observations indicate that the water-soluble graphene is similar to single graphene sheets peeled off from pyrolytic graphite. We observed graphene oxide sheets with lateral sizes of several hundred nanometers to 30 μm.

The elemental compositions of the EDTA-modified graphene were characterized with energy dispersive X-Ray spectroscopy (EDXS). The presence of silicon on EDTA-GO and EDTA-RGO (Figure 5c and 5d) was confirmed by the appearance of the Si

signal at 1.82 KeV. In addition, variation of the EDXS count ratio of carbon to oxygen is a reflection of the stepwise nature of the modification process. As shown in Figure 5c, a higher EDXS count ratio of oxygen to carbon was observed on EDTA-GO, indicating the presence of epoxy groups. Upon reduction with hydrazine, the strength of the oxygen signal decreased compared to that of carbon, as shown in Figure 5d. These results confirmed the conversion of graphene oxide into graphene after reduction with hydrazine and that most epoxy groups had been removed during the reduction process. The same phenomenon was also observed with the signal strength of sodium from EDTA-GO and EDTA-RGO, potentially because some sodium cations were adsorbed on the hydrophilic surface of GO. In contrast, after reduction with hydrazine, the signal strength of sodium decreased compared with that of carbon. These results suggest that sodium cannot be adsorbed on the hydrophobic surface and that the sodium cations were from the EDTA group itself. These data also confirmed the presence of the sodium and COOH groups.
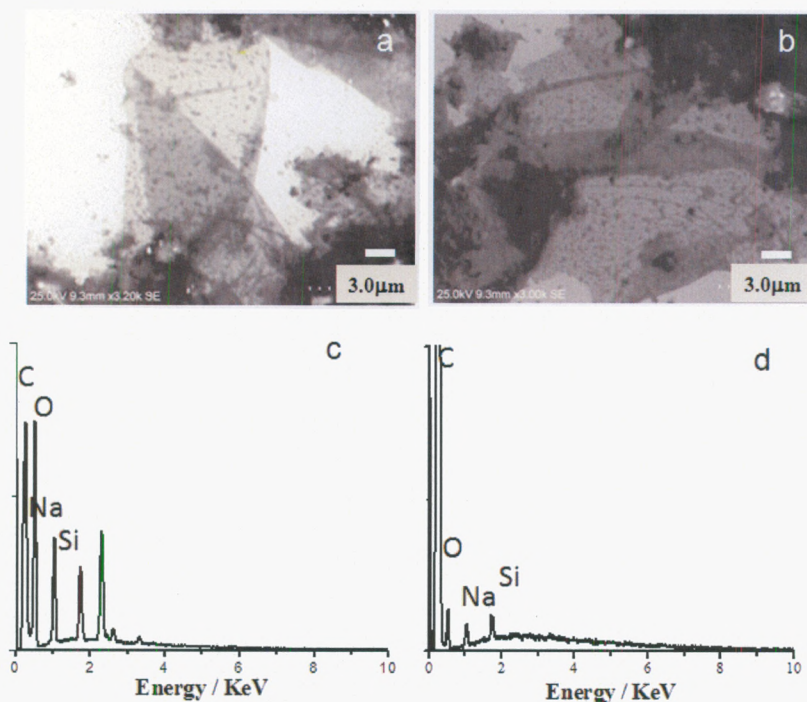
Figure 5. The SEM images of EDTA-GO single sheet (a), EDTA-RGO single sheet (b) and EDXS spectra of EDTA-GO (c) and EDTA-RGO (d).

3.2 Adsorptions properties towards Pb^{2+}

3.2.1 Adsorption Capacities of Pb^{2+}

In a typical experiment to detect the adsorption capacity of EDTA-GO adsorbent for Pb(II), 20 mg of EDTA-GO was mixed with 100 mL of pH 7.2 Pb(II) solution with various concentrations. The solution was left overnight and then vacuum filtered rapidly with a 0.2 μm membrane. The metal ion concentration in the filtrate was determined by AA, UV-Vis and ICP. Figure 6 shows the adsorption isotherms of Pb(II) at its initial concentration range of 0.005~0.1 mg/ml. Pb(II) is more favorably adsorbed on EDTA-GO and the adsorption capacity of Pb(II) attained 535 mg/g at a equilibrium concentration of 0.22 mg/mL, while the adsorption capacity for Pb(II) at GO was 360 mg/g. These results are much higher that than obtained from activated carbon and nitric acid treated CNTs.
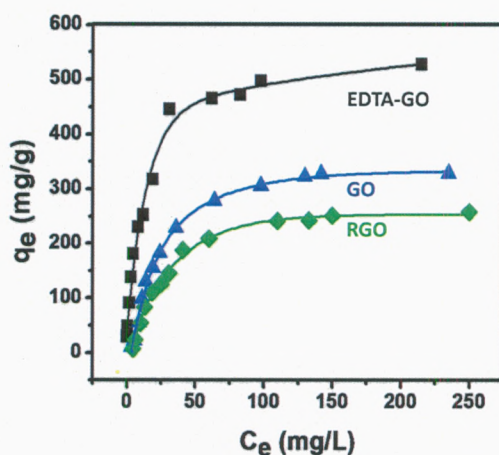

Figure 6. Adsorption Isotherms of Pb(II) onto EDTA-GO (black line), GO (blue line) and RGO (green line) surface. Experiment conditions: Initial concentration 5~100ppm;

sample dose: 20 mg/ 100mL; pH 7.2; temperature 20 °C; contact time 12 hours.

The experimental data for metal ions adsorption onto GO were analyzed using the Langmuir adsorption isotherm model.

The Langmuir adsorption isotherm model is applicable to highly heterogeneous surfaces. This model relates the adsorption of molecules on the surface of the adsorbent to a concentration at a fixed temperature. The Langmuir equation states that:

$$q_e = \frac{q_{max}C_e}{K_l + C_e} \qquad (3)$$

From the linear form of this isotherm, the Langmuir equation can be written as follows:

$$\frac{1}{q_e} = \frac{1}{q_{max}} + \frac{1}{q_{max} \times K_l C_e} \qquad (4)$$

where q_e is the adsorption amount of metals on adsorbent (mg/g), q_{max} is the adsorption capacity of metals on adsorbent (mg/g), C_e is the equilibrium concentration of metals (mg/g), and K_l is the Langmuir adsorption constant, which is related to the adsorption energy. The value for K_l increases as the adsorption binding energy increases with the decrease in temperature.
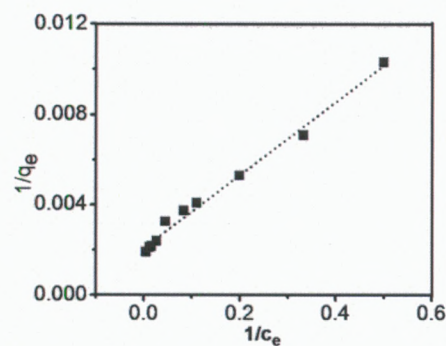
Figure 7. Linearized Langmuir model for Pb(II)

adsorption by EDTA-GO at room temperature

It can be seen from Figure 7 that the Langmuir model shows good agreement with the experimental data, with the correlation coefficient values (R^2 values) of 0.975 at pH 7. The parameter for q_{max} is 486 mg/g, which is related to the adsorption capacity that increases with pH values.

Another model that is used in this investigation is the Freundlich adsorption isotherm.   This model relates the concentration of a solute on the surface of the adsorbent, to the concentration of the solute in a liquid solution.   For Freundlich model, the equation is (5):

$$q_e = K_f C_e^{\frac{1}{n}} \quad (5)$$

where q_e is the adsorption amount of metals on adsorbent (mg/g), C_e is the equilibrium concentration of metals (mg/g),   and K_f and n are Freundlich constants related to adsorption capacity and adsorption intensity, respectively.

From the linear form of this isotherm, the Langmuir equation can be written as follows:

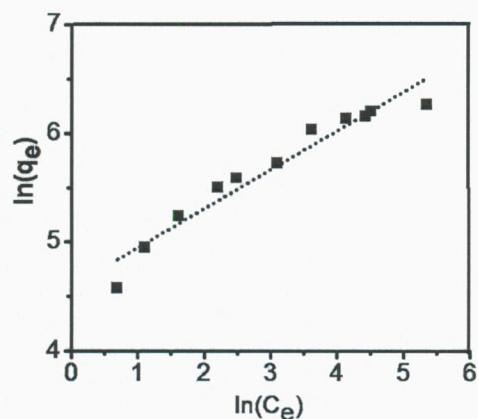$$\log q_e = \log K_f + \frac{1}{n}\log C_e \quad (6)$$

Figure 8. Linearized Freundlich model for Pb(II)

adsorption by EDTA-GO at room temperature

Also, our investigation demonstrates that Freundlich model fit the results with correlation coefficient values of 0.933 (Fig. 6 and Table 1.), which is lower than that of Langmuir models. So the Langmuir models show good agreement with the experimental data, with the high correlation coefficient values of 0.975. These results demonstrate that a monolayer adsorption process and each adsorptive site, such as –COOH, -OH and EDTA groups, can be occupied by heavy metals ions only once in a one-to-one manner. The maximum adsorption capacities of Pb(II) on EDTA-GO and GO are 486 mg/g and 367 mg/g respectively. These values are greater than that of most carbon-based nanomaterials such as oxidized carbon nanotubes and activated carbon. This result is due to the surface area and functional groups on GO surface. The oxidation process of graphite during the synthesis of GO process introduces large amounts of oxygen functional groups such as –OH, -COOH and C=O onto the GO surface and most importantly, the introduction of EDTA groups onto GO surface for chelating heavy metal ions further increases the capacity of GO to hold onto heavy metals.

Table 1. Values of the parameter associated with Langmuir and Frundlich Models

	Langmuir Model			Frundlich Model		
	Q_e (mg/g)	K_l(L/mg)	R^2	K_F (mg/g(mg/l)^n)	n	R^2
EDTA-GO	486	0.122	0.975	71.66	2.27	0.933
GO	367	0.035	0.92	10.69	1.29	0.80
RGO	278	0.031	0.98	7.38	1.35	0.75

3.2.2 Adsorption kinetics

Figure 9 shows the results from UV Spectroscopy after a sample of EDTA-GO was treated with 0.5 mg/mL Pb(II). Two different vials containing 2.3 mg of EDTA-GO were mixed with 20 mL of 0.5 mg/mL Pb(II). Two different methods of exposing the EDTA-GO to the lead solution were performed to see if the type of exposure has any effect on kinetics. One solution was mixed physically in the scintillation vial and the other solution was mixed by sonication. The mixing of these solutions occurred for 15 minutes, then the solution was allowed to sit on the bench top. UV Spectroscopy samples were taken at different time intervals to determine how much Pb^{2+} ions have been adsorbed by the EDTA-GO.

Even at the 5 minute interval, both sonicated solutions have a better adsorption capability than the non-sonicated solution by a significant amount. However, as time passed, the Pb^{2+} ions were able to adsorb to the entire surface of EDTA-GO. After two

hours, both solutions reached a plateau and proved that the maximum capability for the EDTA-GO mixture to adsorb Pb^{2+} ions from the aqueous solution was at around 100%. This proves that the sonication of EDTA-GO with $PbCl_2$ only increases its adsorption capability in an immediate short term effect. After about 2 hours of exposure to the solution, the 100% adsorption will still occur whether or not sonication was the method used to mix the solutions (Figure 9).
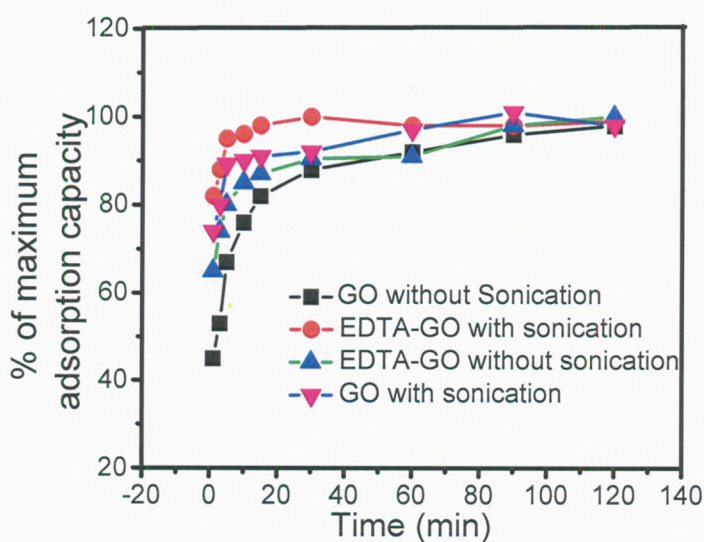

Figure 9. Graphical representation of the adsorption capability of EDTA-GO measured after different time intervals.

3.2.3 Effect of pH on adsorption capacity

After testing the maximum adsorbtion capacity of Pb^{2+} ions, the pH level of the solution was varied to see the dependence of the adsorption capacity. Five scintillation vials containing about 2.3 mg of EDTA-GO were mixed with varying pH levels (3, 4.5, 5.5, 7 and 9). Figure 10 shows the effect of pH on the ability of the EDTA-GO mixture to adsorb Pb^{2+} ions. These data are based on a standard curve of Pb^{2+} ion adsorption. The data was analyzed by UV-Vis spectroscopy and translated into this graph.
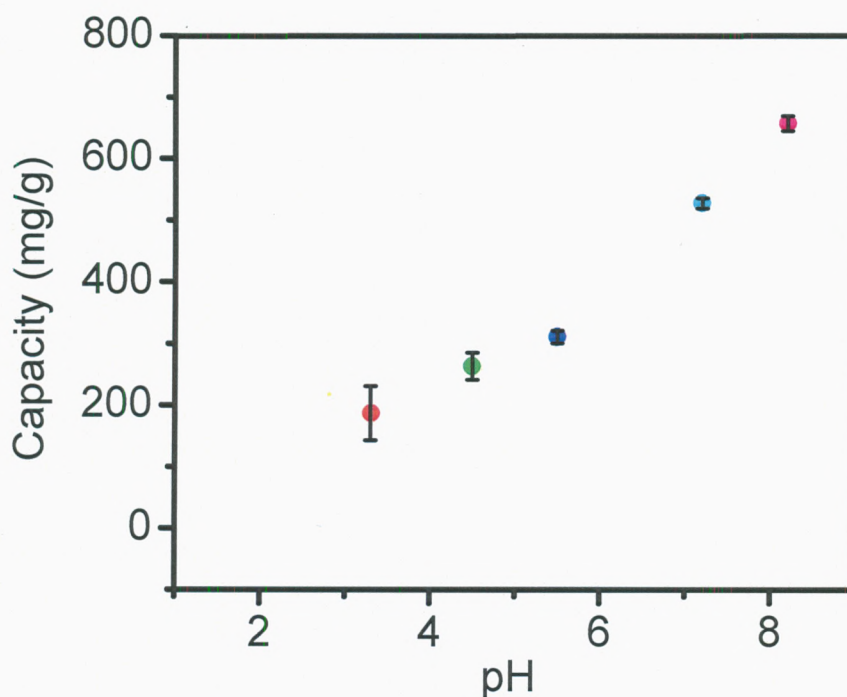
Figure 10. Graphical representation of the adsorption capability of EDTA-GO measured at different pH levels.

Adsorption of Pb^{2+} ions steadily increase as pH increases. This is due to the absence of H^+ ions that are normally present at low pH levels. This absence allows for the carboxyl groups on the ends of the EDTA-GO sheets to attract the Pb^{2+} ions in the solution. The less abundant the H^+ ions are, the surface of EDTA-GO allows for more binding of the carboxyl groups to the heavy metal ions. The pH range selected is important to know because at much lower pH levels than 3, the EDTA-GO-M complex is not very stable. Any higher than 8 and Pb(II) ions are more likely to form the $Pb(OH)_2$ complex.

3.3 EDXS Analysis of Graphene, GO and EDTA-GO with Pb^{2+} ion treatment

Graphene, GO and EDTA-GO were all exposed to Pb(II) to observe their adsorption capacities. All three samples were analyzed through SEM and EDXS. The samples were run before and after exposure to $PbCl_2$. Each spectra shows intensity in units of cps/eV, which is the amount of energy the instrument has measured in over a certain time, on the y-axis. On the x-axis, the peaks shown in the spectra are related to an element's $K\alpha$ value. The $K\alpha$ of an element is defined as the strongest x-ray spectral line observed when exposed to enough energy for maximum x-ray emission. In Figure 11, the EDXS spectra show three standard samples of graphene, GO and EDTA-GO. These samples exhibit the atomic composition of the sample that is being analyzed by EDXS. Graphene shows a strong peak for carbon and nothing else. EDTA-GO has peaks for C, O, and Si to represent how EDTA is bonded to GO. GO has C and O and some background noise peaks that are insignificant to be noted as the presence of another element.
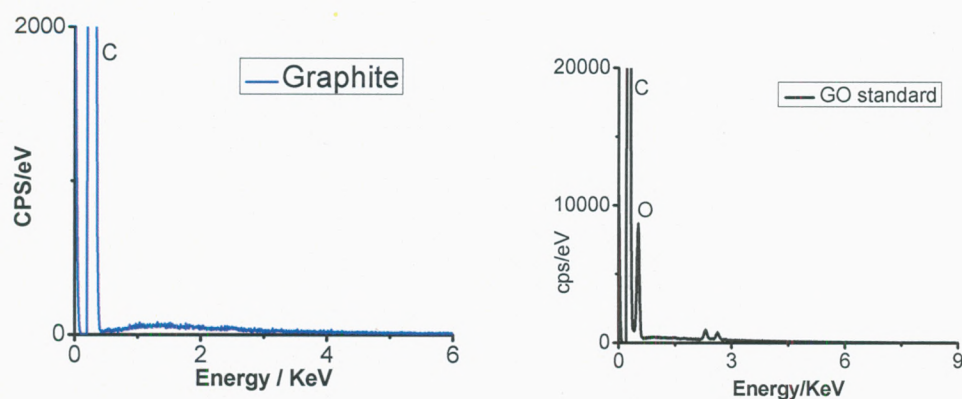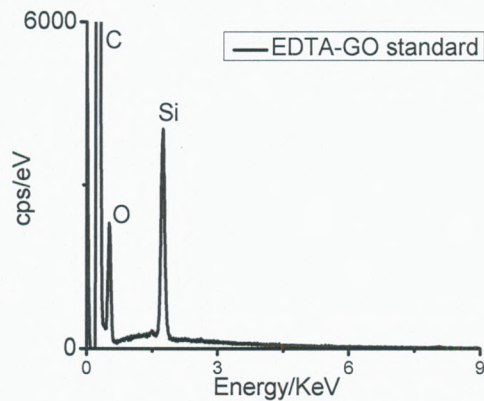
Figure 11. EDXS spectra of Graphene, GO and EDTA-GO before exposure to Pb^{2+} ions.
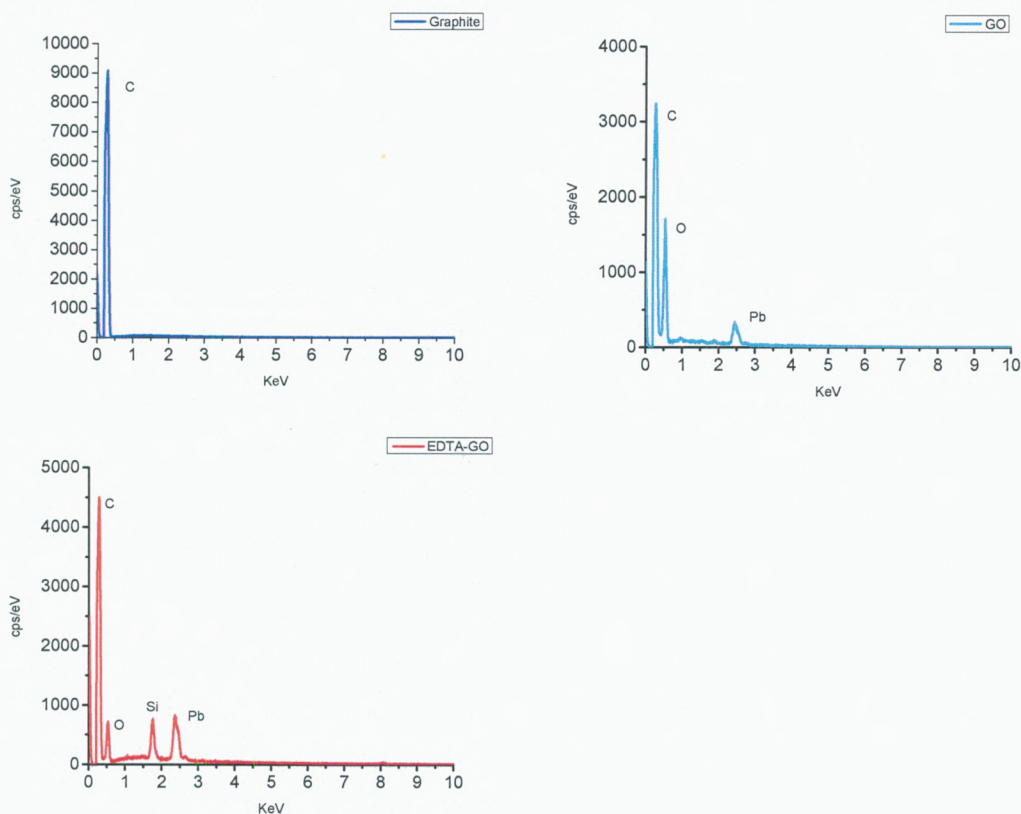

Figure 12. EDXS spectra of Graphene, GO and EDTA-GO after exposure to Pb^{2+} ions.

These same layers of graphene, GO and EDTA-GO were then exposed to 1 mg/mL Pb(II) and left on the bench top overnight to react. The layers were then dried and analyzed through SEM and EDXS (Figure 12). The graphs show that graphene with

no functionalization has no capability to adsorb any lead. This is expected, since there are no O-groups available on the surface to attract any heavy metal ions. On the other hand, GO and EDTA-GO have significant peaks indicating the presence of lead on the surface of the adsorbent layer. The ability of EDTA-GO to be able to adsorb lead is visibly much higher compared to the ability of GO.

Now that the layers can be applied to adsorb heavy metals, a desorption experiment was done on the samples and then analyzed by EDXS again to be properly evaluated if the sample can be reused. The desorption experiment was done by washing the sample with 0.1 M HCl while running through a vacuum filter. The acid restores the metal salt, leaving the complex back to its original state. Figure 13a and 13b show the EDXS result after washing the EDTA-GO and GO layers with HCl.
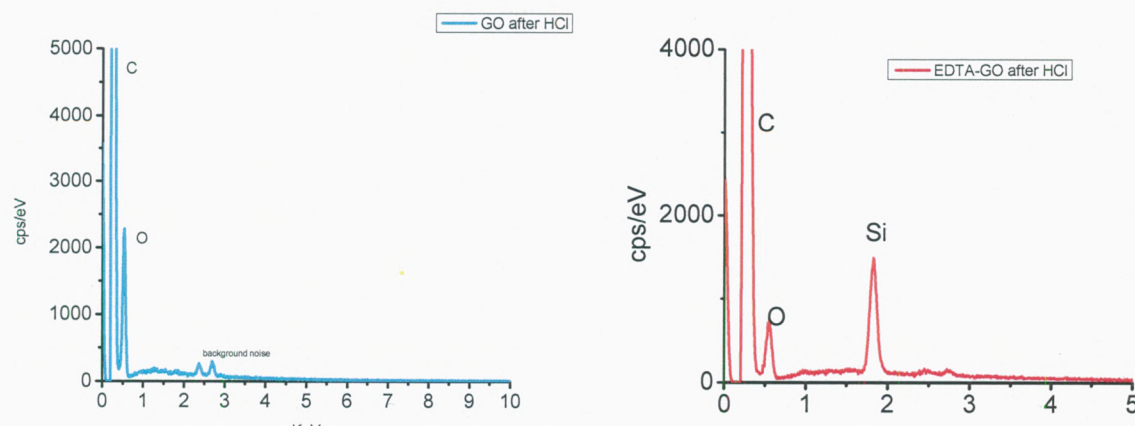

Figure 13. EDXS spectra of GO (a) and EDTA-GO (b) after applying HCl

Both samples clearly confirm that after treatment with only 0.1M HCl, there is a very little presence of Pb(II) ions on the surface of either GO or EDTA-GO. This proves that it is possible to reuse the EDTA-GO layer after being exposed to a solution of Pb(II) ions. The ability of EDTA-GO to be "recycled" makes it a very economical material to

be used repeatedly when adsorbing Pb(II) ions or other divalent heavy metals in aqueous solutions. This is an exciting development for a material that is able to adsorb Pb(II) ions and then release these ions after washing with an acidic solution. A summary of the experiments can be seen in Figure 14. By proving that these graphene derivatives are reusable, it is definitely an area of great interest due to its environmental impact and economic feasibility.
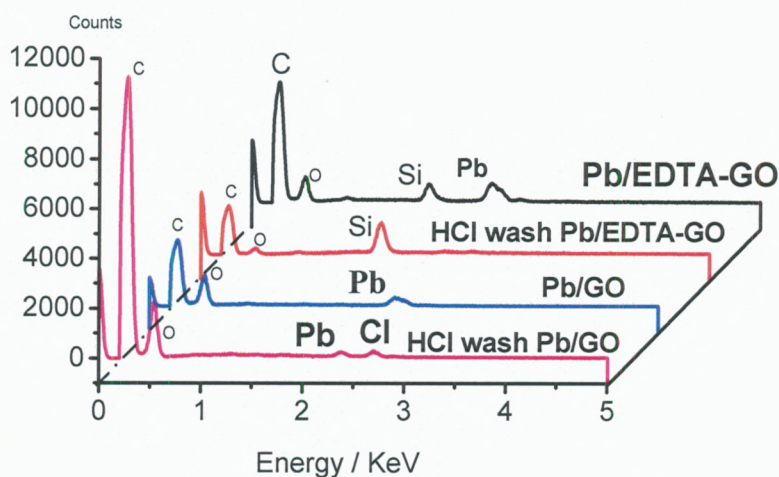

Figure 14. A graphical representation of the summary of EDTA-GO and GO adsorption and desorption experiments.

3.4 GO and EDTA-GO Adsorption With Other Divalent Heavy Metals

Aside from lead, there are other heavy metals present in the environment that is a cause for water pollution. Our investigation led to the study of other heavy metals that can also possibly be adsorbed by the EDTA-GO complex. The adsorption capacities of EDTA-GO for Ca^{2+}, Cd^{2+}, Co^{2+}, Cu^{2+}, Mg^{2+}, Ni^{2+} were tested. To do so, we prepared solutions that contained ions of Ca^{2+}, Cd^{2+}, Co^{2+}, Cu^{2+}, Mg^{2+}, Ni^{2+} each with a

concentration of 1 mg / 1 mL from their respective metal salts. About 0.01 g of EDTA-GO samples were treated with 100 μL of 1 mg/mL of these different metals, and then the treated sample was analyzed through SEM and EDX. The same exact experiment was done for GO as a point of comparison. The EDX spectra for each sample was averaged and compiled into a graph. The graph shows the atomic weight percent of the metal in the sample. This amount was calculated by a method in the EDX program that would estimate the percent composition of an element by weight from the data from its scans. Using these data, we are able to estimate the amount of a certain heavy metal that is present on the surface of the EDTA-GO. The averages from six scans per sample were used to come up with the data for the graphs.
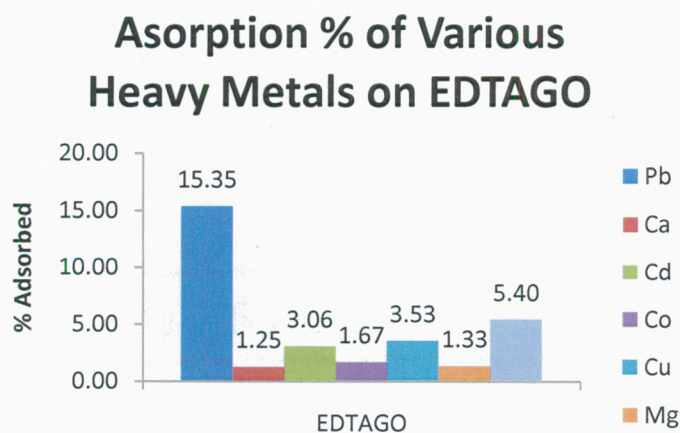
Asorption % of Various Heavy Metals on EDTAGO

Figure 15. A graphical representation of how the adsorption of Pb(II) ions compare to the adsorption of various metals on the surface EDTA-GO.

In comparison to the GO surface, the amount of heavy metals on the surface that is adsorbed by EDTA-GO is significantly higher than the capacity of GO, as expected (Table 2). The amount of Pb(II) present on either sample is considerably greater than the amounts of the other heavy metals adsorbed on the surface of the graphene derivative.

Although the other metals were not adsorbed as much as lead, the amounts on the surface are certainly comparable to other studies done in adsorbing these metals through other techniques.

Table 2. Average results of At. Wt % calculated by EDX after 6 scans / element

At. Wt. %	Pb	Ca	Cd	Co	Cu	Mg	Ni
Before HCl							
EDTA-GO	15.35	1.25	3.06	1.67	3.53	1.33	5.40
GO	12.82	1.13	2.63	1.46	2.91	0.32	1.35
After HCl							
EDTA-GO	1.16	0	0	0	0	0	0
GO	2.35	0	0	0	0	0	0

3.5 Competing substrates for EDTA-GO surface

In an effort to simulate a real-world environment, a mixture of 0.01 mg and 100 µL of each of the heavy metals that have been analyzed were added to a scintillation vial and left overnight. SEM and EDX analysis were done on the sample after drying overnight. The EDX data (Table 3) shows that in comparison to the individual adsorption calculations done, the results showed a significant drop in the capability for EDTA-GO to adsorb lead (Table 2). This suggests that among these heavy metals, there is a competition for the surface of EDTA-GO. As our research shows, lead is still being adsorbed more easily than the other metals.

Table 3. Average results of At. Wt % calculated by EDX after 6 scans

At. Wt. %	Pb	Ca	Cd	Co	Cu	Mg	Ni
EDTA-GO	10.61	1.55	2.32	2.6	0.91	0.63	2.28

Conclusion

Heavy metal contamination in our water resources is very prevalent and needs to be remediated. This kind of pollution negatively affects a lot of industries that require clean freshwater, especially the food industry. Many different techniques are being implemented to remove heavy metal contamination from our water systems however adsorption is one of the most efficient and economically favored processes that is available. Because of its ease in functionalization and modification, graphene has been the adsorbent of choice for this project. We oxidized graphene to establish functional groups on its surface in order to greatly increase its adsorption capabilities. We have silylated GO with EDTA and synthesized EDTA-GO. EDTA-GO was treated with Pb(II) and analyzed using UV-Vis, SEM and EDX to measure its adsorption capability. The data fit the Langmuir and Freundlich models for sorption isotherms, and the resulting data showed that EDTA-GO has a maximum adsorption capacity of 535 mg/g, compared to the maximum GO adsorption capacity at 360 mg/g. The maximum adsorption capacity of EDTA-GO is much higher than activated carbon or oxidized CNTs. EDTA-GO was also exposed to other heavy metals to investigate its adsorption capability. It was able to successfully adsorb a small amount of the heavy metals it was exposed to (Ca^{2+}, $Cd^{2+,}$ Co^{2+}, Cu^{2+}, Mg^{2+} and Ni^{2+}), but it had a significantly higher affinity for lead. Our investigation proves that this novel compound, EDTA-GO, can be further developed and researched to enhance its already astounding abilities to adsorb lead, and hopefully begin a trend in the removal of heavy metal pollution in our water resources in the future.

Acknowledgements:

References:

1) Tuzen, Mustafa, Kadriye O. Saygi, and Mustafa Soylak. "Solid Phase Extraction of Heavy Metal Ions in Environmental Samples on Multiwalled Carbon Nanotubes." *Journal of Hazardous Materials* 152.2 (2008): 632-39.

2) Ekmekyapar, F., A. Aslan, Y. Bayhan, and A. Cakici. "Biosorption of Copper(II) by Nonliving Lichen Biomass of Cladonia Rangiformis Hoffm." *Journal of Hazardous Materials* 137.1 (2006): 293-98.

3) Sublet, R., M. Simonnot, A. Boireau, and M. Sardin. "Selection of an Adsorbent for Lead Removal from Drinking Water by a Point-of-use Treatment Device." *Water Research* 37.20 (2003): 4904-912.

4) Stafiej, A., and K. Pyrzynska. "Adsorption of Heavy Metal Ions with Carbon Nanotubes."*Separation and Purification Technology* 58.1 (2007): 49-52.

5) Wang, H., A. Zhou, F. Peng, H. Yu, and L. Chen. "Adsorption Characteristic of Acidified Carbon Nanotubes for Heavy Metal Pb(II) in Aqueous Solution." *Materials Science and Engineering: A* 466.1-2 (2007): 201-06.

6) Sekar, M., V. Sakthi, and S. Rengaraj. "Kinetics and Equilibrium Adsorption Study of Lead(II) onto Activated Carbon Prepared from Coconut Shell." *Journal of Colloid and Interface Science* 279.2 (2004): 307-13.

7) Sekar, M., V. Sakthi, and S. Rengaraj. "Kinetics and Equilibrium Adsorption Study of Lead(II) onto Activated Carbon Prepared from Coconut Shell." *Journal of Colloid and Interface Science* 279.2 (2004): 307-13.

8) Chen, Junyi, Dongqiang Zhu, and Cheng Sun. "Effect of Heavy Metals on the Sorption of Hydrophobic Organic Compounds to Wood Charcoal." *Environmental Science & Technology* 41.7 (2007): 2536-541.

9) Brown, Pauline, I. Atly Jefcoat, Dana Parrish, Sarah Gill, and Elizabeth Graham. "Evaluation of the Adsorptive Capacity of Peanut Hull Pellets for Heavy Metals in Solution." *Advances in Environmental Research* 4 (2000): 19-29

10) Li, Qingbiao. "Simultaneous Biosorption of Cadmium (II) and Lead (II) Ions by Pretreated Biomass of Phanerochaete Chrysosporium." *Separation and Purification Technology* 34.1-3 (2004): 135-42

11) Tuzen, M., K. Saygi, C. Usta, and M. Soylak. "Pseudomonas Aeruginosa Immobilized Multiwalled Carbon Nanotubes as Biosorbent for Heavy Metal Ions." *Bioresource Technology* 99.6 (2008): 1563-570.

12) Narasimhulu, Korrapati, and Parcha Sreenivasa Rao. "Studies On Removal of Toxic Metals From Wastewater Using Pseudomonas Species." *ARPN Journal of Engineering and Applied Sciences* 4.7 (2009): 63-58.

13) Seredych, Mykola, and Teresa J. Bandosz. "Adsorption of Ammonia on Graphite Oxide/aluminium Polycation and Graphite Oxide/zirconium–aluminium Polyoxycation Composites." *Journal of Colloid and Interface Science* 324.1-2 (2008): 25-35.

14) Choi, Moonjung, and Jyongsik Jang. "Heavy Metal Ion Adsorption onto Polypyrrole-impregnated Porous Carbon." *Journal of Colloid and Interface Science* 325.1 (2008): 287-89.

15) Li, Jing, Shaojun Guo, Yueming Zhai, and Erkang Wang. "High-sensitivity Determination of Lead and Cadmium Based on the Nafion-graphene Composite Film." *Analytica Chimica Acta*649.2 (2009): 196-201

16) Malakootian, M., J. Nouri, and H. Hossaini. "Removal of Heavy Metals from Paint Industry's Wastewater Using Leca as an Available Adsorbent." *Int. J. Environ. Sci. Tech* 6.2 (2009): 183-190.

17) Jin, Li. "Mechanisms of Lead Adsorption on Chitosan/PVA Hydrogel Beads." *Langmuir* 18.25 (2002): 9765-770.

18) Lu, Chungsying, Huantsung Chiu, and Chunti Liu. "Removal of Zinc(II) from Aqueous Solution by Purified Carbon Nanotubes: Kinetics and Equilibrium Studies." *Industrial & Engineering Chemistry Research* 45.8 (2006): 2850-855.

19) Zhou, Dong-Mei, Yu-Jun Wang, Han-Wei Wang, Shen-Qiang Wang, and Jie-Min Cheng. "Surface-modified Nanoscale Carbon Black Used as Sorbents for Cu(II) and Cd(II)." *Journal of Hazardous Materials* 174 (2009): 34-39.

20) Ganjali, Mohammad Reza, Negar Motakef-Kazami, Farnoush Faridbod, Sepideh Khoee, and Parviz Norouzi. "Determination of Pb^{2+} Ions by a Modified Carbon Paste Electrode Based on Multi-walled Carbon Nanotubes (MWCNTs) and Nanosilica." *Journal of Hazardous Materials* 173 (2009): 415-19.

21) Li, Yan-Hui, Jun Ding, Zhaokun Luan, Zechao Di, Yuefeng Zhu, Cailu Xu, Dehai Wu, and Bingqing Wei. "Competitive Adsorption of Pb, Cu and Cd Ions from Aqueous Solutions by Multiwalled Carbon Nanotubes." *Carbon* 41 (2003): 2787-792.

22) Agnihotri, S., M. Rood, and M. Rostamabadi. "Adsorption Equilibrium of Organic Vapors on Single-walled Carbon Nanotubes." *Carbon* 43.11 (2005): 2379-388.

23) Dai, Hongjie. "Carbon Nanotubes: Synthesis, Integration, and Properties." *ChemInform* 34.8 (2003).

24) Wang, Hongjuan, Ailin Zhou, Feng Peng, Hao Yu, and Jian Yang. "Mechanism Study on Adsorption of Acidified Multiwalled Carbon Nanotubes to Pb(II)." *Journal of Colloid and Interface Science* 316.2 (2007): 277-83.

25) Sun, D., X. Xie, Y. Cai, H. Zhang, and K. Wu. "Voltammetric Determination of Cd^{2+} Based on the Bifunctionality of Single-walled Carbon Nanotubes–Nafion Film." *Analytica Chimica Acta* 581.1 (2007): 27-31.

26) Haubner, Kinga, Jan Murawski, Phillip Olk, Lukas M. Eng, Christoph Ziegler, Barbara Adolphi, and Evelin Jaehne. "The Route to Functional Graphene Oxide." *ChemPhysChem* 11 (2010): 2131-139.

27) Mkhoyan, K. Andre, Alexander W. Contryman, John Silcox, Derek A. Stewart, Goki Eda, Cecilia Mattevi, Steve Miller, and Manish Chhowalla. "Atomic and Electronic Structure of Graphene-Oxide." *Nano Letters* 9.3 (2009): 1058-063.

28) Wang, Lu, Kyuho Lee, Yi-Yang Sun, Michael Lucking, Zhongfang Chen, Ji Jun Zhao, and Shengbai B. Zhang. "Graphene Oxide as an Ideal Substrate for Hydrogen Storage." *ACS Nano* 3.10 (2009): 2995-3000.

29) Gilje, Scott, Song Han, Minsheng Wang, Kang L. Wang, and Richard B. Kaner. "A Chemical Route to Graphene for Device Applications." *Nano Letters* 7.11 (2007): 3394-398.

30) Si, Yongchao, and Edward T. Samulski. "Synthesis of Water Soluble Graphene." *Nano Letters* 8.6 (2008): 1679-682.

31) Hartono, Tri, Shaobin Wang, Qing Ma, and Zhonghua Zhu. "Layer Structured Graphite Oxide as a Novel Adsorbent for Humic Acid Removal from Aqueous Solution." *Journal of Colloid and Interface Science* 333.1 (2009): 114-19.

32) Seredych, M., C. Petit, A. Tamashausky, and T. Bandosz. "Role of Graphite Precursor in the Performance of Graphite Oxides as Ammonia Adsorbents." *Carbon* 47.2 (2009): 445-56.

33) Barroso-Bujans, F., S. Cerveny, R. Verdejo, J.J. Del Val, J.M. Alberdi, A. Alegria, and J. Colmenero. "Permanent Adsorption of Organic Solvents in Graphite Oxide and Its Effect on the Thermal Exfoliation." *Carbon* 48 (2010): 1079-087.

34) Savage, Nora, and Mamadou S. Diallo. "Nanomaterials and Water Purification: Opportunities and Challenges." *Journal of Nanoparticle Research* 7.4-5 (2005): 331-42.

35) Berger, Michael. "Nanotechnology and Water Treatment." *Nanotechnology and Nanoscience | Nanowerk*. Nanowerk, LLC, 22 Feb. 2008. Web. 27 Apr. 2011. <http://www.nanowerk.com/spotlight/spotid=4662.php>.

36) Geim, Andre K., and Philip Kim. "Carbon Wonderland: Scientific American." *Science News, Articles and Information | Scientific American*. Scientific American, 17 Mar. 2008. Web. 27 Apr. 2011. <http://www.scientificamerican.com/article.cfm?id=carbon-wonderland>.

37) Gómez-Navarro, Cristina, R. Thomas Weitz, Alexander M. Bittner, Matteo Scolari, Alf Mews, Marko Burghard, and Klaus Kern. "Electronic Transport Properties of Individual Chemically Reduced Graphene Oxide Sheets." *Nano Letters* 7.11 (2007): 3499-503.

Publications and Presentations

1. Formation of Highly Stable Dispersions of Silane-functionalized Reduced Graphene Oxide. Shifeng Hou, Shujun Su, Marc Kasner, <u>Robert D. Cuellari</u>, <u>P. Shah</u>,<u>K. Patel</u>, <u>C. J. Madarang</u>, Chemical Physics Letters, Volume 501, Issues 1-3, 6 December 2010, Pages 68-74.

2. Adsorption Behavior of EDTA-graphene oxide for Pb (II) and Heavy Metal Pollutant Removal, Submitted to *ACS Applied Materials & Interfaces*.

3. Adsorption Behavior of EDTA-graphene oxide for Pb (II) and Heavy Metal Pollutant Removal. Nanotech, June 2011, Boston